

Bis(8-hydroxyquinolinato)platinum 7,7,8,8-Tetracyanoquinodimethane, Pt(QNL)₂·TCNQ. Synthesis, Structure and Spectroscopic Properties

P. BERGAMINI, V. BERTOLASI, V. FERRETTI and S. SOSTERO*

Department of Chemistry, University of Ferrara, Via Borsari 46, 44100 Ferrara, Italy

(Received July 28, 1986)

Abstract

The title complex, Pt(QNL)₂·TCNQ, was prepared by the reaction of Pt(QNL)₂ with TCNQ in acetonitrile. This complex consists of stacks of alternating, parallel Pt(QNL)₂ and TCNQ molecules. The molecules of Pt(QNL)₂ and TCNQ in the stack are planar and nearly parallel. The angle between the mean plane defined by the phenyl ring in TCNQ and the mean plane defined by the atoms Pt, O₁, O₁', N₁ and N₁' is 3.57°. The Pt(QNL)₂·TCNQ is diamagnetic. The visible spectrum exhibits a charge transfer band at 10 100 cm⁻¹ indicating that there is some charge-transfer interaction in the complex. Spectroscopic data and the analysis of the bond distances in the TCNQ moiety indicates that the degree of charge-transfer in Pt(QNL)₂·TCNQ is small.

Introduction

Molecular 'charge-transfer complexes' between various organic electron donors and acceptors have been known for some time and their broad range of fascinating properties have been widely studied [1, 2]. There are, however, many fewer examples of charge-transfer complexes derived from transition metal compounds and organic acceptors. Formation of these complexes is assisted if the donors and acceptors are planar, conjugated molecules. 8-Hydroxyquinolinato complexes [3] of transition metals have an ideal structure for forming charge-transfer complexes with the powerful electron acceptor tetracyanoquinodimethane.

Our interest in charge-transfer complexes involving Pt(II) complexes stems from previous studies [4] on spectroscopy and photophysics of bis(8-hydroxyquinolinato)platinum(II) compound, denoted as Pt(QNL)₂. The complex (Pt(QNL)₂) is intensely luminescent in solutions at room temperature. This property, coupled with its broad absorption spec-

trum, makes it a potential candidate as an electron and energy transfer process sensitizer in solution.

In the present paper, the preparation, structure and optical properties of the 1:1 charge-transfer complex, Pt(QNL)₂·TCNQ are reported.

Experimental

Preparation of Pt(QNL)₂·TCNQ (I)

Pt(QNL)₂ was prepared as described previously [5]. 7,7,8,8-Tetracyanoquinodimethane (TCNQ) was purchased from Aldrich Chemicals. TCNQ (2 mmol) in hot acetonitrile was added to a solution of Pt(QNL)₂ (2 mmol) in boiling acetonitrile. The reaction mixture was stirred and refluxed for 30 min after which time the volume was reduced by half. Upon cooling to room temperature complex I was obtained. Crystals of I, suitable for diffraction study, were grown in an H-tube by running together a chloroform solution of Pt(QNL)₂ and an acetonitrile solution of TCNQ. Elemental analysis for complex I was performed by Alfred Bernarht Laboratories and gave results corresponding to a 1:1 stoichiometry. *Anal.* Calc. for C₃₀H₁₆N₆O₂Pt: C, 52.40; H, 2.34; N, 12.22; Pt, 28.37. Found: C, 52.46; H, 2.33; N, 12.20; Pt, 28.35%. The 1:1 stoichiometry was later confirmed by X-ray structure determination.

Instrumentation

Visible and near infrared spectra were obtained with a Perkin-Elmer 323 recording spectrophotometer. Infrared spectra were recorded with a Perkin-Elmer Model 283B spectrophotometer. Solid samples were examined in KBr pellets and as Nujol mulls between KBr plates.

Magnetic susceptibility measurements were carried out by the Faraday method. Electron paramagnetic resonance measurements were made at room temperature and 77 K on both single crystal and powder samples using a Bruker ER 200 D spectrometer. Emission spectrum was recorded on a Perkin-Elmer

* Author to whom correspondence should be addressed.

TABLE I. Crystal Data

Formula weight	687.59
Crystal size (mm)	0.1 × 0.2 × 0.24
Space group	$P\bar{1}$
Unit cell parameters (Å)	$a = 8.146(1), b = 8.262(2),$ $c = 9.701(2)$
and (°)	$\alpha = 102.96(2), \beta =$ $107.35(1), \gamma = 79.22(2)$
V (Å ³)	602.2(2)
Z	1
$F(000)$	332
ρ (calc.) (g cm ⁻³)	1.89
ρ (obs.) (g cm ⁻³)	1.92
μ (Mo K α) (cm ⁻¹)	59.2
Radiation	Mo K α
Monochromator	graphite
θ_{\min} – θ_{\max}	2–30°
Standard reflections	3 (stable)
Temperature (°C)	22
No. independent reflections	3516
No. with $I > 3\sigma(I)$	3423
No. variables (last cycle)	210
Final R_1^a, R_2^a	0.023, 0.027
Final shift/error maximum	0.15
Largest peak (e Å ⁻³) in the final difference map	0.61
Weighting	$1/w^2 = 1/\sigma^2(I) + 0.041$
Error in an observation of unit weight	0.91

$$^a R_1 = \sum |\Delta F_o| / \sum |F_o|, R_2 = (\sum w |\Delta F_o|^2 / \sum w |F_o|^2)^{1/2}.$$

MPF-3 spectrofluorimeter. Lifetime measurements were determined by laser flash photolysis as previously described.

X-ray Diffraction

Crystal data (see Table I) were collected on an Enraf-Nonius CAD-4 diffractometer with monochromated Mo K radiation and $\omega/2\theta$ scan technique. Cell parameters were obtained by least-squares methods from the refined setting angles of 25 reflections in the range 9°–14°. Intensities were corrected for Lorentz, polarization and absorption (minimum transmission factor of 74.1). Scattering factors and anomalous dispersion parameters were taken from the International Tables for X-ray Crystallography [9]. The position of the platinum atom was found by Patterson synthesis and all other non-H atoms were located in the subsequent Fourier map. The H atoms were located in the Fourier maps after a few cycles of isotropic refinement. Finally, the structure was refined by full matrix least-squares using anisotropic temperature factors for all non-H atoms and isotropic for hydrogens. Weights for the last cycle were applied according to the scheme given in Table I. All calculations were performed by SDP [10] and PARST [11] systems of programs.

TABLE II. Positional ($\times 10^4$) and Thermal Parameters (Å²) with e.s.d.s in Parentheses

Atom	x	y	z	B_{eq}^a/B
Pt	0	0	0	2.091(2)
O(1)	791(3)	906(3)	-1423(2)	2.84(4)
N(1)	631(3)	-2179(3)	-1217(3)	2.35(4)
C(1)	1263(3)	-303(3)	-2435(3)	2.41(5)
C(2)	1816(4)	-56(4)	-3583(3)	2.86(5)
C(3)	2289(4)	-1411(4)	-4596(3)	3.19(6)
C(4)	2239(4)	-3054(4)	-4514(3)	3.17(6)
C(5)	1678(4)	-3363(4)	-3373(3)	2.70(5)
C(6)	1560(5)	-4976(4)	-3154(4)	3.46(6)
C(7)	1002(5)	-5131(4)	-2001(4)	3.71(6)
C(8)	540(4)	-3705(4)	-1042(3)	3.16(5)
C(9)	1192(3)	-1992(3)	-2357(3)	2.22(4)
H(2)	1805(52)	1140(50)	-3697(45)	3.5(9)
H(3)	2626(48)	-1223(47)	-5417(41)	2.7(7)
H(4)	2601(56)	-3935(56)	-5205(48)	4.0(9)
H(6)	1946(53)	-5959(53)	-3770(45)	3.6(8)
H(7)	918(62)	-6297(61)	-1866(54)	4.8(11)
H(8)	169(52)	-3693(52)	-91(44)	3.4(8)
N(2)	3860(6)	5694(5)	1977(4)	5.06(9)
N(3)	3019(5)	2024(5)	4216(3)	4.64(7)
C(10)	4484(4)	1317(4)	1058(3)	2.76(5)
C(11)	5000(4)	1660(4)	-128(3)	2.78(5)
C(12)	4506(4)	-421(4)	1141(3)	2.79(5)
C(13)	3974(4)	2590(4)	2087(3)	2.82(5)
C(14)	3924(5)	4325(4)	2033(4)	3.47(6)
C(15)	3461(4)	2274(4)	3278(4)	3.41(4)
H(11)	4991(54)	2853(53)	-185(46)	3.7(9)
H(12)	4165(51)	-603(51)	1951(43)	3.2(8)

$$^a B_{\text{eq}} = (4/3) \sum_i \sum_j a_i a_j \beta_{ij}.$$

Final positional and equivalent isotropic vibrational parameters are given in Table II. Bond distances and angles are given in Tables III and IV. Tables of observed and calculated structure factors have been deposited as supplementary material.

Results and Discussion

Structure

The crystal is built up by stacks of alternating TCNQ and Pt(QNL)₂ molecules situated around centers of symmetry, (0, 0, 0) for Pt(QNL)₂ and ($\frac{1}{2}, 0, 0$) for TCNQ, along the crystallographic a axis and separated by ~ 3.5 Å. The molecules of TCNQ and Pt(QNL)₂ are planar and are nearly parallel, the angle between the mean plane defined by the phenyl ring in TCNQ and the mean plane defined by the atoms Pt, O₁, O₁', N₁, N₁' being 3.57(8)°. The molecules of TCNQ and Pt(QNL)₂ are shown in Figs. 1 and 2, and the molecular overlap along the a axis is shown in Fig. 3.

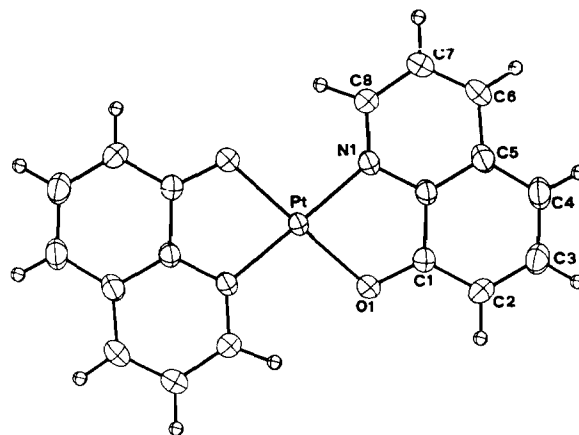
This packing is typical of systems which present semi-conducting properties owing to the charge-

TABLE III. Interatomic Distances (Å) with e.s.d.s in Parentheses

Pt—O(1)	2.014(3)	N(2)—C(14)	1.135(6)
Pt—N(1)	1.990(2)	N(3)—C(15)	1.144(6)
O(1)—C(1)	1.323(3)	C(10)—C(11)	1.435(5)
N(1)—C(8)	1.328(4)	C(10)—C(12)	1.453(5)
N(1)—C(9)	1.364(5)	C(10)—C(13)	1.374(4)
C(1)—C(2)	1.386(5)	C(11)—C(12')	1.344(4)
N(1)—C(9)	1.364(5)	C(13)—C(14)	1.439(5)
C(1)—C(2)	1.386(5)	C(13)—C(15)	1.429(6)
C(1)—C(9)	1.427(4)		
C(2)—C(3)	1.392(4)	C(11)—H(11)	1.00(4)
C(3)—C(4)	1.386(5)	C(12)—H(12)	0.96(5)
C(4)—C(5)	1.404(5)		
C(5)—C(6)	1.420(5)		
C(5)—C(9)	1.406(4)		
C(6)—C(7)	1.365(6)		
C(7)—C(8)	1.395(4)		
C(2)—H(2)	1.02(4)		
C(3)—H(3)	0.97(5)		
C(4)—H(4)	0.94(4)		
C(6)—H(6)	0.96(4)		
C(7)—H(7)	1.02(5)		
C(8)—H(8)	1.05(4)		

TABLE IV. Bond Angles (°) with e.s.d.s in Parentheses

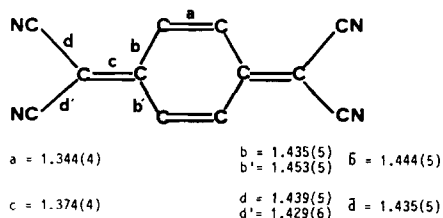
O(1)—Pt—N(1)	82.2(1)	C(11)—C(10)—C(12)	118.2(3)
Pt—O(1)—C(1)	111.8(2)	C(11)—C(10)—C(13)	121.3(3)
Pt—N(1)—C(8)	127.8(2)	C(12)—C(10)—C(13)	120.6(3)
Pt—N(1)—C(9)	112.7(2)	C(10)—C(11)—C(12')	121.6(3)
C(8)—N(1)—C(9)	119.5(3)	C(10)—C(12)—C(11')	120.3(3)
O(1)—C(1)—C(2)	124.9(3)	C(10)—C(13)—C(14)	122.1(3)
O(1)—C(1)—C(9)	118.2(2)	C(10)—C(13)—C(15)	122.1(3)
C(2)—C(1)—C(9)	117.0(3)	C(14)—C(13)—C(15)	115.8(3)
C(1)—C(2)—C(3)	120.7(3)	N(2)—C(14)—C(13)	179.0(4)
C(2)—C(3)—C(4)	122.5(3)	N(2)—C(15)—C(13)	178.7(4)
C(3)—C(4)—C(5)	118.8(3)		
C(4)—C(5)—C(6)	124.9(3)	C(10)—C(11)—H(11)	118(2)
C(4)—C(5)—C(9)	118.6(3)	C(12')—C(11)—H(11)	120(2)
C(6)—C(5)—C(9)	116.5(3)	C(10)—C(12)—H(12)	116(2)
C(5)—C(6)—C(7)	120.0(3)	C(11')—C(12)—H(12)	124(3)
C(6)—C(7)—C(8)	120.0(3)		
N(1)—C(8)—C(7)	121.6(3)		
N(1)—C(9)—C(1)	115.1(2)		
N(1)—C(9)—C(5)	122.5(3)		
C(1)—C(9)—C(5)	122.5(3)		
C(1)—C(2)—H(2)	118(2)		
C(3)—C(2)—H(2)	121(2)		
C(2)—C(3)—H(3)	120(2)		
C(4)—C(3)—H(3)	118(2)		
C(3)—C(4)—H(4)	120(3)		
C(5)—C(4)—H(4)	121(3)		
C(5)—C(6)—H(6)	120(3)		
C(7)—C(6)—H(6)	120(3)		
C(6)—C(7)—H(7)	119(3)		
C(8)—C(7)—H(7)	121(3)		
C(7)—C(8)—H(8)	126(2)		
N(1)—C(8)—H(8)	112(2)		

Fig. 1. An ORTEP [20] view of the Pt(QNL)₂ moiety showing the thermal ellipsoids at 40% probability.

transfer derived from a molecule donor and a TCNQ acceptor [1, 6].

Molecular Geometry of the TCNQ Molecule and an Estimate of the Degree of Charge-Transfer

Comparing the bond distances of the present structure with several other TCNQ species [1, 6] it is observed that the TCNQ molecule displays a typical quinoid structure indicating a low or very low charge-transfer in this system. The degree of charge-transfer can be calculated from structural data using the method performed by Kristenmacher *et al.* [7] which estimates this degree by means of the ratio $c/(b+d)$ (see Scheme 1).



Scheme 1.

Bond distances are very similar to those found [8] in TCNQ and the ratio $c/(b+d)$, equal to 0.477, suggests a very low degree of charge-transfer in this system (no charge-transfer corresponds to a ratio = 0.476, while charge-transfer of one electron, e.g. TCNQ⁻, to a ratio = 0.5). The latter ratio is in good correlation with the degree of charge-transfer based on other physical properties (see spectroscopic properties).

Spectroscopic Properties

Infrared data. The infrared spectrum of **I** is essentially a superimposition of the spectrum of the individual neutral component molecules. However, as a result of the molecular association, there are small

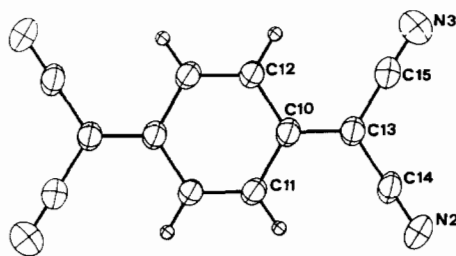


Fig. 2. An ORTEP [20] view of the TCNQ moiety showing the thermal ellipsoids at 40% probability.

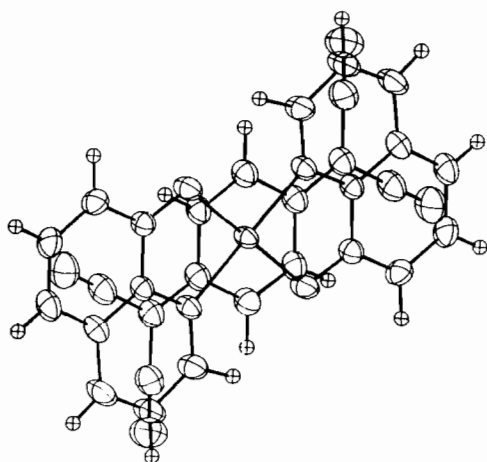


Fig. 3. An ORTEP [20] view of the $\text{Pt}(\text{QNL})_2 \cdot \text{TCNQ}$ complex showing the thermal ellipsoids at 40% probability.

differences in frequencies and intensities of some bands:

(i) The two most intense bands [12] of free TCNQ (C-H bending mode, 864 cm^{-1} and $\text{C}(\text{CN})_2$ wagging mode, 475 cm^{-1}) are shifted to lower frequencies (830 and 460 cm^{-1}) in adduct **I**. These effects may be related to the face-to-face packing of $\text{Pt}(\text{QNL})_2$ and TCNQ molecules.

(ii) The $\text{C}\equiv\text{N}$ stretching frequency is found at 2228 cm^{-1} in TCNQ and at 2220 cm^{-1} in **I**, a shift comparable to that observed for several other neutral TCNQ π complexes [13]. The absence of bands in the $2200\text{--}2180 \text{ cm}^{-1}$ region [14], where the $\text{C}\equiv\text{N}$ stretching modes of TCNQ^- appear, indicates there are no significant exchange interactions.

Magnetic Properties

Bulk magnetic susceptibility measurements show **I** to be diamagnetic. This is in keeping with the absence of EPR signals for **I** at either room temperature or 77 K . These points indicate that the degree of charge-transfer in **I** between the donor molecule $\text{Pt}(\text{QNL})_2$ and the electron acceptor TCNQ is very small, in agreement with the IR data and structural results.

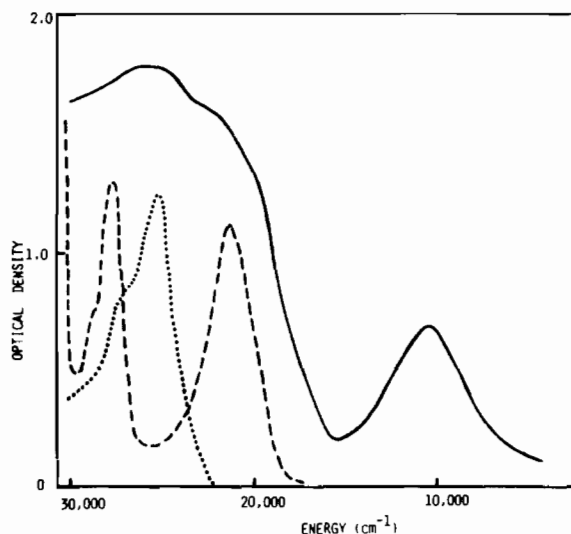


Fig. 4. Visible and near-infrared spectra: (—) $\text{Pt}(\text{QNL})_2 \cdot \text{TCNQ}$ in a KBr pellet; (---) $\text{Pt}(\text{QNL})_2$ in acetonitrile; (.....) TCNQ in acetonitrile.

Electronic Absorption Data

The solid-state electronic spectrum of **I** in the $30\,000\text{--}5\,000 \text{ cm}^{-1}$ region is shown in Fig. 4 along with the solution spectra of the isolated donor $\text{Pt}(\text{QNL})_2$ and acceptor TCNQ compounds. The spectrum is composed of the sum of the neutral component molecule spectra. A broad band at $10\,100 \text{ cm}^{-1}$ appears in the low energy region, where neither of the component molecules absorb. This low energy band can be assigned as intermolecular charge-transfer transition from $\text{Pt}(\text{QNL})_2$ to TCNQ in the π complex **I** on the basis of the following considerations:

(i) For a series of organometals acting as donors toward a single acceptor the energy of the charge-transfer band is proportional to the ionization potential of the donor [15,16]. The solid-state charge-transfer band of the $\text{Pd}(\text{QNL})_2 \cdot \text{TCNQ}$ complex [17] ($11\,500 \text{ cm}^{-1}$) is close in energy to the **I** charge-transfer band so it appears that the ionization potentials of $\text{Pd}(\text{QNL})_2$ and $\text{Pt}(\text{QNL})_2$ are very similar [3].

(ii) For the common donor $\text{Pt}(\text{QNL})_2$ the difference in charge-transfer band frequencies are mainly caused by the difference in the electron affinity (E_a) [16] of the acceptor molecules. The charge-transfer band of $\text{Pt}(\text{QNL})_2 \cdot \text{TCNE}$ is located [17] at $14\,300 \text{ cm}^{-1}$. Thus, the difference in the charge-transfer energies ($h\nu_{\text{CT}} \text{Pt}(\text{QNL})_2 \cdot \text{TCNQ} - h\nu_{\text{CT}} \text{Pt}(\text{QNL})_2 \cdot \text{TCNE} = 0.42 \text{ eV}$) agree well with the $E_a(\text{TCNQ}) - E_a(\text{TCNE}) = 0.4 \text{ eV}$ [18, 19].

(iii) The solid-state luminescence spectrum of **I** ($15\,200 \text{ cm}^{-1}$) is close in energy to that of $\text{Pt}(\text{QNL})_2$ [4]. This is in keeping with its assignment to a spin forbidden $d\text{--}d$ transition as is its energy [4]. Although perceptibly lower than the value for the

free [4] Pt(QNL)₂ (8.05 μs in cellulose acetate film) the luminescence lifetime ($\tau = 3.8 \mu\text{s}$ at 22 °C) indicates a weak quenching effect exerted by the TCNQ molecule.

Results (i), (ii) and (iii) are consistent with a system in which the intermolecular forces between adjacent molecules in stack I are weak compared to the intramolecular bonding of the component molecules Pt(QNL)₂ and TCNQ. Within the limits of the very weak interactions observed and the close contacts ($\sim 3.5 \text{ \AA}$) of adjacent molecules in the stack, the absorption band at $10\,100 \text{ cm}^{-1}$ can be attributed to contact charge-transfer (CCT) which can be approximated by the electron transfer process itself [16].

Although Pt(QNL)₂·TCNQ overlap region does include the Pt atom, the Pt–TCNQ distances are too large to permit significant interaction between the π orbital of TCNQ and the d_{z^2} orbital of the Pt atom. Consequently the CT band at $10\,100 \text{ cm}^{-1}$ is probably the result of electron transfer from the filled oxinate orbitals to an occupied TCNQ π^* orbital.

Acknowledgements

We gratefully acknowledge Professors G. Gilli and O. Traverso for valuable discussions and suggestions.

References

- 1 F. H. Herbstcin, *Perspect. Struct. Chem.*, **4**, 166–395 (1971).
- 2 R. Foster, 'Molecular Complexes', Vol. 1, Cranc, Russak, New York, 1973; Vol. 2, 1974.
- 3 A. S. Bailey, R. J. P. Williams and J. D. Wright, *J. Chem. Soc.*, 2579 (1965).
- 4 C. Bartocci, S. Sostero, O. Traverso, A. Cox, T. J. Kemp and J. W. Reed, *J. Chem. Soc., Faraday Trans. I*, **76**, 797 (1980).
- 5 R. Ballardini, M. T. Indelli, G. Varani, C. A. Bignozzi and F. Scandola, *Inorg. Chim. Acta*, **31**, L423 (1978).
- 6 S. Flandrois and D. Chasseau, *Acta Crystallogr., Sect. B*, **33**, 2744 (1977).
- 7 T. J. Kristenmacher, T. J. Emge, A. N. Bloch and D. O. Cowan, *Acta Crystallogr., Sect. B*, **38**, 1193 (1982).
- 8 R. E. Long, R. A. Sparks and K. N. Trueblood, *Acta Crystallogr.*, **18**, 932 (1965).
- 9 D. T. Cromer and J. T. Waber, 'International Tables for X-ray Crystallography', Vol. IV, Kynoch Press, Birmingham, U.K., 1974.
- 10 B. A. Frenz, in H. Schenk, R. Olthof-Hazekamp, H. Von Koningsveld and G. C. Bassi (eds.), 'Computing in Crystallography', University Press, Delft, 1978, p. 47–71.
- 11 M. Nardelli, *Comput. Chem.*, **7**, 95 (1983).
- 12 A. Girlando and C. Pecile, *Spectrochim. Acta, Part A*, **29**, 1859 (1973).
- 13 M. Z. Siegmund, *Z. Chem.*, **15**, 194 (1975).
- 14 R. Bozio, A. Girlando and C. Pecile, *J. Chem. Soc., Faraday Trans.*, **2**, 1237 (1975).
- 15 R. S. Mulliken and W. B. Person, *Ann. Rev. Phys. Chem.*, **13** 107 (1982).
- 16 M. Tamres and J. Grundness, *J. Am. Chem. Soc.*, **93**, 801 (1971).
- 17 P. Bergamini, S. Sostero and O. Traverso, unpublished results.
- 18 C. D. Cooper and R. N. Compton, *J. Chem. Phys.*, **66**, 4325 (1977).
- 19 L. D. Palmer and L. E. Lyons, *Aust. J. Chem.*, **29**, 1919 (1976).
- 20 C. K. Johnson, 'ORTEP', Report ORNL-3794, revised, Oak Ridge National Laboratory, Tenn., 1971.